SCIENCE CHINA
Information Sciences

• RESEARCH PAPER •

February 2018, Vol. 61 022304:1–022304:13
doi: 10.1007/s11432-016-9053-3

Partial intersection sphere decoding with weighted voting for sparse rotated V-OFDM systems

Qi FENG[1*], Xiang-Gen XIA[2,3] & Naitong ZHANG[1,4]

[1]*School of Electronic Science and Engineering, Nanjing University, Nanjing* 210023*, China;*
[2]*College of Information Engineering, Shenzhen University, Shenzhen* 518060*, China;*
[3]*Department of Electrical and Computer Engineering, University of Delaware, Newark DE* 19716*, USA;*
[4]*School of Electronics and Information Engineering, Harbin Institute of Technology, Harbin* 150001*, China*

Received 18 September 2016/Revised 30 December 2016/Accepted 15 February 2017/Published online 24 August 2017

Abstract Vector orthogonal frequency division multiplexing (V-OFDM) is a general system that builds a bridge between OFDM and single-carrier frequency domain equalization in terms of intersymbol interference level and receiver complexity. In this paper, we focus on a rotated V-OFDM system over a broadband sparse channel owing to its large time delay spread and fewer nonzero taps. In order to collect the multipath diversity, a simple rotation matrix is designed, independent of the number of subchannels at the transmitter. For the rotated V-OFDM receiver, a partial intersection sphere decoding with weighted voting method is proposed by exploiting the sparse nature of the multipath channel. The proposed receiver chooses the transmitted vector from the set with the maximum likelihood estimation generated using the partial intersection sphere decoding method. For an extreme case, such as when a candidate set is empty, which usually occurs at a low signal-to-noise ratio (SNR), an efficient weighted voting system is used to estimate the transmitted vectors symbol-by-symbol. Simulation results indicate that the proposed receiver improves the symbol error rate performance with reduced complexity, especially for low SNR scenarios.

Keywords vector orthogonal frequency division multiplexing, sparse multipath channel, partial intersection sphere decoding, weighted voting, diversity order

Citation Feng Q, Xia X-G, Zhang N T. Partial intersection sphere decoding with weighted voting for sparse rotated V-OFDM systems. Sci China Inf Sci, 2018, 61(2): 022304, doi: 10.1007/s11432-016-9053-3

1 Introduction

Orthogonal frequency division multiplexing (OFDM) is a promising multicarrier transmission scheme, and it has been widely adopted in broadband wireless communications and radar applications [1–5]. Although OFDM reduces demodulation complexity at a receiver, it cannot collect the multipath diversity, and thus, its performance is worse than that of single-carrier frequency domain equalization (SC-FDE) [6–8]. However, SC-FDE suffers from unbalanced complexities between a transmitter and receiver [9, 10]. Therefore, OFDM is more suitable for downlink transmission with high data rate, while SC-FDE can be applied for uplink transmission that reduces peak-to-average power ratio [2].

Vector orthogonal frequency division multiplexing (V-OFDM) for a single antenna converts an ISI channel into multiple vector subchannels, where the vector size is a predesigned parameter [11]. On one hand, V-OFDM reduces either the cyclic prefix (CP) overhead or the inverse fast Fourier transform (IFFT) size with respect to a single antenna OFDM system. On the other hand, V-OFDM has a lower

* Corresponding author (email: xiaoyehouzi@126.com)

decoding complexity at the receiver compared with SC-FDE. Therefore, V-OFDM is a general system that builds a bridge between OFDM and SC-FDE. For V-OFDM, an adaptive vector channel allocation scheme was proposed in [12]. Some key techniques in V-OFDM systems, such as carrier/sampling-frequency synchronization and guard-band configuration, were compared with the conventional OFDM system [13]. Iterative demodulation and decoding under turbo principle is an efficient way to reduce the complexity of V-OFDM receiver [14]. Instead of the conventional quasi-static model, V-OFDM systems over fast fading channels were investigated, and the intercarrier interference between different vectors were derived [15]. Phase noise impairment in V-OFDM systems was compensated, and the expectation-maximization algorithm was proposed [16, 17]. A V-OFDM system may not be able to collect the full multipath diversity for all subchannels with the maximum likelihood (ML) receiver, and constellation rotated V-OFDM (CRV-OFDM) overcomes this drawback [18–20]. With a certain rotation of the constellation, all the subchannels can achieve full multipath diversity, and their symbol error rate (SER) performances are almost the same as those obtained with the ML receiver. It should be noted that in [21], it was shown that the linear minimum mean square error (MMSE) receiver can perform a tradeoff between multipath diversity and decoding complexity.

This study focuses on a rotated V-OFDM system, which is a special type of CRV-OFDM, over a broadband sparse channel owing to its large time delay spread and fewer nonzero taps [22, 23]. For a sparse multipath channel, most entries in a blocked channel matrix of rotated V-OFDM are zero and the nonzero entries are regularly placed. Thus, sparse nonzero entries can be extracted efficiently and possible symbol sequences lying in a sphere can be searched, which can significantly reduce the complexity of rotated V-OFDM over an entire channel. Based on the above idea, a partial intersection sphere decoding with weighted voting (PIS-WV) method is proposed for a rotated V-OFDM system. Unlike the ML decoding method that requires the enumeration of symbol constellation, the proposed PIS-WV receiver chooses the transmitted vector only from the set of candidate vectors generated by the partial intersection sphere (PIS) decoding method with the minimum distance. For an extreme case, such as when a candidate set is empty, which usually occurs at a low signal-to-noise ratio (SNR), the weighted voting system is used to estimate the transmitted symbols with the knowledge of PIS decoding. The proposed PIS-WV decoding method can achieve a good symbol error rate (SER) performance with reduced complexity, especially for low SNR scenarios.

2 System model

A rotated V-OFDM system is a generalization of an OFDM system where scalar sequences are vectorized and multiplied by a rotation angle. As shown in Figure 1, we first introduce the rotated V-OFDM system for a single transmission antenna. In general, symbol sequences in a V-OFDM system are processed block-by-block, which is similar to a conventional OFDM system, except that the V-OFDM system further divides each block into several vectors.

In a V-OFDM system, N modulated symbols $\boldsymbol{X} = [X_0, X_1, \ldots, X_{N-1}]^{\mathrm{T}}$ are blocked into L column vectors with size of M, where $(\cdot)^{\mathrm{T}}$ denotes the transpose. It is assumed that the average power is normalized, i.e., $\mathbb{E}\left\{\left|X_n^2\right|\right\} = 1,\ n = 0, 1, \ldots, N-1$, where $\mathbb{E}\{\cdot\}$ represents mathematical expectation. $\boldsymbol{X}_l$ is denoted as the lth transmitted vector in $\boldsymbol{X}$, i.e.,

$$\boldsymbol{X}_l = [X_{lM}, X_{lM+1}, \ldots, X_{lM+M-1}]^{\mathrm{T}}, \quad l = 0, 1, \ldots, L-1. \tag{1}$$

In order to collect multipath diversity, $\boldsymbol{X}_l$ needs to be specifically rotated [18], and a few optimal angles for diagonal cyclotomic space-time codes derived in [24] can be applied. As the proposed PIS-WV decoding method can be directly adopted for any rotated V-OFDM system with full diversity, in this study, a simple rotation matrix is designed, independent of the number of subchannels, such that all the transmitted vectors are passed through the same rotation matrix in parallel, i.e, $\widetilde{\boldsymbol{X}_l} = \boldsymbol{\Phi}_M \boldsymbol{X}_l$, where

$$\boldsymbol{\Phi}_M = \mathrm{diag}\left\{1, \mathrm{e}^{-\mathrm{j}\frac{\pi}{N}}, \ldots, \mathrm{e}^{-\mathrm{j}\frac{\pi}{N}(M-1)}\right\}. \tag{2}$$

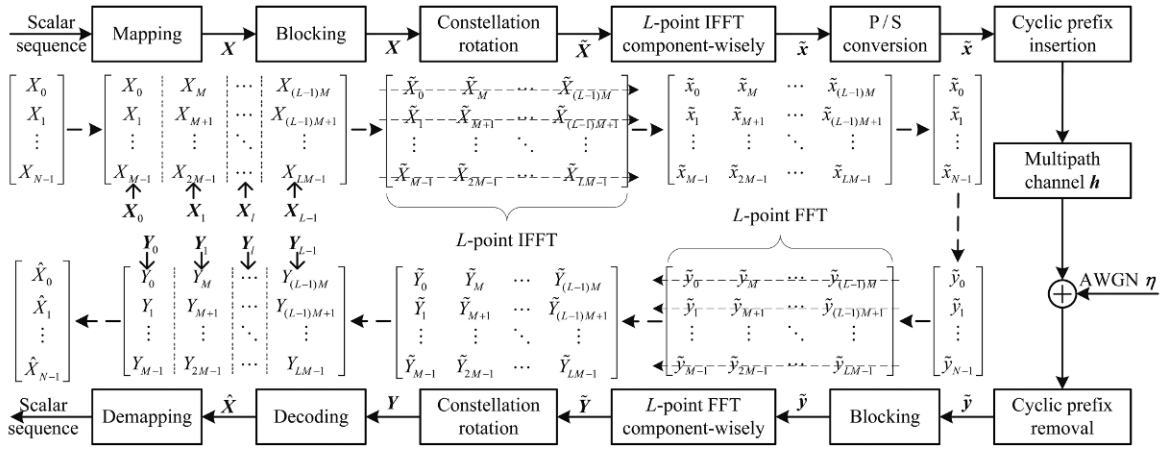

Figure 1 The block diagram of a rotated V-OFDM modulation system.

As we will see in the simulations later, with the proposed parallel rotation, all L subchannels can collect full diversity with the proposed PIS-WV decoding method, and the difference in performance between the rotation in [18] and the designed simple rotation in (2) is small. Furthermore, $\widetilde{\boldsymbol{x}}_k = [\widetilde{x}_{kM}, \widetilde{x}_{kM+1}, \ldots, \widetilde{x}_{kM+M-1}]^{\mathrm{T}}$ is the normalized component-wise vector L-point IFFT of $\widetilde{\boldsymbol{X}}_l$, i.e.,

$$\widetilde{\boldsymbol{x}}_k = \frac{1}{\sqrt{L}} \sum_{l=0}^{L-1} \widetilde{\boldsymbol{X}}_l \mathrm{e}^{\mathrm{j}\frac{2\pi}{L}kl}, \quad k = 0, 1, \ldots, L-1. \tag{3}$$

After parallel to serial (P/S) conversion, the transmitted symbol sequence $\widetilde{\boldsymbol{x}} = \left[\widetilde{\boldsymbol{x}}_0^{\mathrm{T}}, \widetilde{\boldsymbol{x}}_1^{\mathrm{T}}, \ldots, \widetilde{\boldsymbol{x}}_{L-1}^{\mathrm{T}}\right]^{\mathrm{T}}$. Γ is denoted as the length of CP, and it should not be shorter than the maximum multipath excess delay of frequency selective fading channel. After inserting CP, the symbol sequence is transmitted serially through the channel arranged with the order $[\widetilde{x}_{N-\Gamma}, \widetilde{x}_{N-\Gamma+1}, \ldots, \widetilde{x}_{N-1}, \widetilde{x}_0, \widetilde{x}_1, \ldots, \widetilde{x}_{N-1}]^{\mathrm{T}}$.

At the receiver, an inverse process to the transmitter is performed accordingly. After removing CP, the received sequence $\widetilde{\boldsymbol{y}} = [\widetilde{y}_0, \widetilde{y}_1, \ldots, \widetilde{y}_{N-1}]^{\mathrm{T}}$ is equal to the circular convolution of the transmitted sequence and the channel impulse response $\boldsymbol{h}$ with additive white Gaussian noise (AWGN) $\boldsymbol{\xi}$, i.e.,

$$\widetilde{y}_n = \widetilde{x}_n \circledast h_n + \xi_n, \quad n = 0, 1, \ldots, N-1, \tag{4}$$

where $\circledast$ denotes circular convolution, the channel impulse response $\boldsymbol{h} = [h_0, h_1, \ldots, h_P]^{\mathrm{T}}$ with the maximum multipath excess delay P, the noise sequence $\boldsymbol{\xi} = [\xi_0, \xi_1, \ldots, \xi_{N-1}]^{\mathrm{T}}$ is independent and identically distributed (i.i.d.), whose entry follows complex Gaussian distribution, i.e., $\xi_n \sim \mathcal{CN}\left(0, \sigma^2\right)$. The received sequence $\widetilde{\boldsymbol{y}}$ is blocked into L column vector $\left[\widetilde{\boldsymbol{y}}_0^{\mathrm{T}}, \widetilde{\boldsymbol{y}}_1^{\mathrm{T}}, \ldots, \widetilde{\boldsymbol{y}}_{L-1}^{\mathrm{T}}\right]^{\mathrm{T}}$, where the kth vector in $\widetilde{\boldsymbol{y}}$ is represented by $\widetilde{\boldsymbol{y}}_k = [\widetilde{y}_{kM}, \widetilde{y}_{kM+1}, \ldots, \widetilde{y}_{kM+M-1}]^{\mathrm{T}}$.

Then, $\widetilde{\boldsymbol{Y}}_l$ is denoted as the normalized L-point component-wise vector FFT of $\widetilde{\boldsymbol{y}}_k$, i.e.,

$$\widetilde{\boldsymbol{Y}}_l = \frac{1}{\sqrt{L}} \sum_{k=0}^{L-1} \widetilde{\boldsymbol{y}}_k \mathrm{e}^{-\mathrm{j}\frac{2\pi}{L}kl}, \quad l = 0, 1, \ldots, L-1. \tag{5}$$

Finally, L column vectors $\widetilde{\boldsymbol{Y}}_l$ are passed through a derotation matrix $\boldsymbol{\Phi}_M^{\mathrm{H}}$ in parallel, i.e., $\boldsymbol{Y}_l = \boldsymbol{\Phi}_M^{\mathrm{H}} \widetilde{\boldsymbol{Y}}_l$, where $(\cdot)^{\mathrm{H}}$ denotes the conjugate transpose. The lth received symbol sequence in $\boldsymbol{Y}$ is represented by $\boldsymbol{Y}_l = [Y_{lM}, Y_{lM+1}, \ldots, Y_{lM+M-1}]^{\mathrm{T}}$. According to [11], the relationship between the lth transmitted vector $\boldsymbol{X}_l$ and received vector $\boldsymbol{Y}_l$ can be derived as

$$\boldsymbol{Y}_l = \boldsymbol{\mathcal{H}}_l \boldsymbol{X}_l + \boldsymbol{\Xi}_l, \quad l = 0, 1, \ldots, L-1, \tag{6}$$

where $\boldsymbol{\mathcal{H}}_l$ is an $M \times M$ block channel matrix, i.e.,

$$\boldsymbol{\mathcal{H}}_l = \begin{bmatrix} H_{l,0} & \mathrm{e}^{-\mathrm{j}\frac{2\pi}{L}(l-\frac{1}{2})}H_{l,M-1} & \cdots & \mathrm{e}^{-\mathrm{j}\frac{2\pi}{L}(l-\frac{1}{2})}H_{l,1} \\ H_{l,1} & H_{l,0} & \cdots & \mathrm{e}^{-\mathrm{j}\frac{2\pi}{L}(l-\frac{1}{2})}H_{l,2} \\ \vdots & \vdots & \ddots & \vdots \\ H_{l,M-2} & H_{l,M-3} & \cdots & \mathrm{e}^{-\mathrm{j}\frac{2\pi}{L}(l-\frac{1}{2})}H_{l,M-1} \\ H_{l,M-1} & H_{l,M-2} & \cdots & H_{l,0} \end{bmatrix}, \tag{7}$$

where $H_{l,m} = \sum_k h_{kM+m}\mathrm{e}^{-\mathrm{j}\frac{2\pi}{L}(kl+\frac{m}{2M})},\ m = 0, 1, \ldots, M-1$, and the additive noise $\boldsymbol{\Xi}_l$ is an i.i.d. complex Gaussian sequence with the same distribution as $\boldsymbol{\xi}_l$. Mathematically, $\boldsymbol{\mathcal{H}}_l$ is a quasi-cyclic matrix (also called pseudo-circulant polynomial matrix), where each entry of the upper triangular part (not including the diagonal) of the circulant matrix is multiplied by a scaled factor, and can be diagonalized as

$$\boldsymbol{\mathcal{H}}_l = \boldsymbol{\Phi}_M^{\mathrm{H}}\boldsymbol{\Lambda}_l^{\mathrm{H}}\boldsymbol{F}_M^{\mathrm{H}}\boldsymbol{H}_l\boldsymbol{F}_M\boldsymbol{\Lambda}_l\boldsymbol{\Phi}_M, \tag{8}$$

where $\boldsymbol{H}_l = \mathrm{diag}\left\{H_l, H_{l+L}, \ldots, H_{l+(M-1)L}\right\}$ and $\boldsymbol{H} = [H_0, H_1, \ldots, H_{N-1}]^{\mathrm{T}}$ is the N-point FFT of zero padded $\boldsymbol{h}$, $\boldsymbol{F}_M$ denotes the $M \times M$ normalized discrete Fourier transform matrix, and $\boldsymbol{\Lambda}_l$ is a diagonal matrix defined as $\mathrm{diag}\left\{1, \mathrm{e}^{-\mathrm{j}\frac{2\pi}{N}l}, \ldots, \mathrm{e}^{-\mathrm{j}\frac{2\pi}{N}(M-1)l}\right\}$.

3 Partial intersection sphere decoding with weighted voting

For a broadband rotated V-OFDM system, a sparse multipath channel $\boldsymbol{h}$ is assumed to have only K nonzero taps with the maximum multipath excess delay P, which is known at the receiver. In order to solve the optimal symbol vector $\boldsymbol{X}_l$ in (6) with the minimum Euclidean distance, the conventional ML receiver needs to enumerate the symbol vector constellation $\mathbb{X}^M$; then, the decoding complexity is exponential to the vector size M. Sphere decoding is a well-known technique to solve the closest lattice point problem, especially for multiple-input multiple-output (MIMO) systems [25, 26]. The basic idea of sphere decoding is computing the QR-decomposition $\boldsymbol{\mathcal{H}}_l = \boldsymbol{Q}\boldsymbol{R}$, where $\boldsymbol{Q}$ is a unitary matrix and $\boldsymbol{R}$ is an upper triangular matrix with positive real-valued entries on its main diagonal [27, 28]. By performing depth-first tree search and pruning, sphere decoding can asymptotically achieve the optimal ML decoding performance with reduced complexity [29, 30].

Motivated by the special structure of the pseudo-circulant channel matrix $\boldsymbol{\mathcal{H}}_l$, we are devoted toward developing an efficient receiver by exploiting the sparse nature of the multipath channel, which does not require the computation of QR-decomposition. Therefore, unlike the sphere decoding method that can be applied to both MIMO and V-OFDM systems, the proposed receiver can only facilitate a V-OFDM system over sparse multipath channel.

Denote $\mathcal{J}$ as the set of time delays of K nonzero taps in a sparse multipath channel $\boldsymbol{h}$, i.e.,

$$\mathcal{J} = \left\{j \middle| j \in \{0, 1, \ldots, P\},\ h_j \neq 0\right\}. \tag{9}$$

Then, the cardinality of the set $\mathcal{J}$ is equal to K, i.e., $|\mathcal{J}| = K$. Considering the special structure of the blocked channel matrix $\boldsymbol{\mathcal{H}}_l$, denote $\mathcal{I}$ as the remainder set of multipath delays modulo vector size M, i.e.,

$$\mathcal{I} = \left\{i \middle| \forall j \in \mathcal{J},\ i = j \bmod M\right\}. \tag{10}$$

Denote κ as the cardinality of the remainder set $\mathcal{I}$, i.e., $\kappa = |\mathcal{I}|$. It should be noted that $\boldsymbol{\mathcal{H}}_l$ is featured by a pseudo-circulant matrix (7) where the number of nonzero entries in each row is equal to κ. As K is small, κ is small as well. Suppose $i_0,\ i_1, \ldots,\ i_{\kappa-1}$ are the κ entries in $\mathcal{I}$ arranged in an ascending order $0 \leqslant i_0 < i_1 < \cdots < i_{\kappa-1} \leqslant M-1$. If K is much less than M when M is large, as in this study, it is not difficult to check that the pseudo-circulant matrix $\boldsymbol{\mathcal{H}}_l$ is sparse. Furthermore, most entries in $\boldsymbol{\mathcal{H}}_l$ are zero and the nonzero entries are regularly placed, i.e., for the mth row, only the $(m-i_0) \bmod M$th, $(m-i_1) \bmod M$th, ... , and $(m-i_{\kappa-1}) \bmod M$th columns are nonzero entries.

Table 1 Notations in partial intersection sphere decoding with weighted voting algorithm

Notation	Definition	Notation	Definition
$\mathcal{J}$	The set of time delays of K nonzero taps in a sparse multipath channel $\boldsymbol{h}$	$\mathcal{I}$	The remainder set of multipath delays modulo vector size M
$\boldsymbol{\mathcal{H}}_l^m$	The $1\times\kappa$ vector extracted from the mth row and the $(m-i_0)$ mod Mth, $(m-i_1)$ mod Mth, $\ldots$, $(m-i_{\kappa-1})$ mod Mth columns of $\boldsymbol{\mathcal{H}}_l$	$\mathcal{S}^m$	The set of κ-dimensional symbol sequences $\boldsymbol{S}$ inside a certain sphere around the mth received signal in $\boldsymbol{Y}_l$
$\mathcal{U}^m$	The set of existing coordinates of the nonzero entries in the first $m-1$ rows of $\boldsymbol{\mathcal{H}}_l$	$\mathcal{V}^m$	The set of current coordinates of the nonzero entries in the mth row of $\boldsymbol{\mathcal{H}}_l$
$\mathcal{W}^m$	The intersection of the existing nonzero coordinates set $\mathcal{U}^m$ and the current nonzero coordinates set $\mathcal{V}^m$	$\mathcal{X}^M$	The set of candidate vectors that the estimation of the transmitted vector $\boldsymbol{X}_l$ would be chosen from
$\mathcal{X}_{\boldsymbol{S}}^m$	The set of symbol sequence in the mth iteration for a given current κ-dimensional $\boldsymbol{S}\in\mathcal{S}^m$	$\mathcal{X}^m$	The set of entire symbol sequence in the mth iteration

Based on the above observation, the κ nonzero entries in each row of $\boldsymbol{\mathcal{H}}_l$ can be efficiently extracted, and all possible κ-dimensional symbol sequences can be searched inside a certain hypersphere around the received signal. Thus, the complexity of searching such possible sequences is exponential to the number of nonzero entries in each row of $\boldsymbol{\mathcal{H}}_l$, which is equal to κ and much less than M. After searching the overall M rows, we can generate a set $\mathcal{X}^M$ of candidate vectors satisfying all M rows, and then choose the transmitted vector from the set $\mathcal{X}^M$ with the maximum likelihood estimation.

If the set $\mathcal{X}^M$ is empty, which usually occurs at low SNR scenarios, a weighted voting system is used to estimate the transmitted vector symbol-by-symbol. The idea of weighted voting is to choose the transmitted vector from the candidate symbols based on the votes they can receive, while each vote should be weighted by the total number of symbol sequences lying in the sphere.

The proposed partial intersection sphere decoding with weighted voting (PIS-WV) method is illustrated in Algorithm 1 and described below in detail. Here, partial intersection means the intersection of the existing and the current nonzero coordinate sets. In each iteration, the proposed PIS decoding method only needs to compare the current symbol sequences corresponding to the coordinates belonging to the partial intersection with the existing ones. To facilitate reading, we have listed the notations of the sets addressed in the PIS-WV decoding method in Table 1. For initialization, the set of existing coordinates of the nonzero entries $\mathcal{U}^0$ and the set of entire symbol sequences $\mathcal{X}^0$ are empty sets, respectively. For each symbol, the initial weighted votes of all candidates $X\in\mathbb{X}$ are set to 0. In the mth iteration with $0\leqslant m\leqslant M-1$, $\mathcal{U}^m$ and $\mathcal{V}^m$ are denoted as the sets of existing coordinates of the nonzero entries in the first $m-1$ rows and current coordinates of the nonzero entries in the mth row of the blocked channel matrix $\boldsymbol{\mathcal{H}}_l$, respectively. Then, the partial intersection $\mathcal{W}^m$ is defined as the intersection of the existing nonzero coordinates set $\mathcal{U}^m$ and the current nonzero coordinates set $\mathcal{V}^m$, i.e., $\mathcal{W}^m=\mathcal{U}^m\bigcap\mathcal{V}^m$. We describe the updating process of generating the set $\mathcal{X}^m$ of possible symbol sequences in the mth iteration with $0\leqslant m\leqslant M-1$ as follows.

(1) Search all possible symbol sequences $\boldsymbol{S}=[S_0,S_1,\ldots,S_{\kappa-1}]^{\mathrm{T}}$, $\boldsymbol{S}\in\mathbb{X}^\kappa$ that lie in the sphere radius r around the received signal Y_{lM+m} and generate the set of symbol sequences $\mathcal{S}^m$ as

$$\mathcal{S}^m=\Big\{\boldsymbol{S}\Big|\boldsymbol{S}\in\mathbb{X}^\kappa,\ \big|Y_{lM+m}-\boldsymbol{\mathcal{H}}_l^m\boldsymbol{S}\big|\leqslant r\Big\},\tag{11}$$

where $\mathbb{X}$ is the constellation of transmitted symbol X_n, Y_{lM+m} is the mth entry of the column vector $\boldsymbol{Y}_l$, $\boldsymbol{\mathcal{H}}_l^m$ is the $1\times\kappa$ vector extracted from the mth row and $(m-i_0)$ mod Mth, $(m-i_1)$ mod Mth, $\ldots$, $(m-i_{\kappa-1})$ mod Mth columns of $\boldsymbol{\mathcal{H}}_l$, where $\boldsymbol{\mathcal{H}}_l$ can be derived from (7).

(2) For each $\boldsymbol{S}\in\mathcal{S}^m$, construct an injective mapping of coordinates $f:\ \ell\to(m-i_\ell)$ mod M, $\ell\in\{0,1,\ldots,\kappa-1\}$. For each symbol sequence $\boldsymbol{X}^m\in\mathcal{X}^m$, where $\mathcal{X}^m$ is the set of entire symbol sequences generated from the previous iteration, compare the current symbol sequence $\boldsymbol{S}$ for the coordinates belonging to the partial intersection $\mathcal{W}^m$ with the existing symbol sequence $\boldsymbol{X}^m$. If $X_w^m=S_{f^{-1}(w)}$ holds for all $w\in\mathcal{W}^m$, where X_w^m stands for the wth entry in $\boldsymbol{X}^m$, then $\boldsymbol{X}^m$ is inserted into the set of symbol sequences $\mathcal{X}_{\boldsymbol{S}}^m$. Insert the symbols whose coordinates belong to the complement of the partial intersection

Algorithm 1 Partial intersection sphere decoding with weighted voting

Input: $\boldsymbol{Y}$, $\boldsymbol{h}$, L, M, P, r
Output: $\widehat{\boldsymbol{X}}$

Initialization: $\mathcal{U}^0 \leftarrow \varnothing,\ \mathcal{X}^0 \leftarrow \varnothing,\ \boldsymbol{\beta} \leftarrow \boldsymbol{0}$;
for $l \leftarrow 0, 1, \ldots, L-1$ **do**
  for $m \leftarrow 0, 1, \ldots, M-1$ **do**
    Y_{lM+m} is the mth entry of column vector $\boldsymbol{Y}_l$;
    $\boldsymbol{\mathcal{H}}_l^m$ is the $1\times\kappa$ vector aligned as the mth row and the $(m-i_0)$ mod Mth, $(m-i_1)$ mod Mth, $\ldots$, $(m-i_{\kappa-1})$ mod Mth columns of $\boldsymbol{\mathcal{H}}_l$;
    Generate a set of κ-dimensional symbol sequences: $\mathcal{S}^m \leftarrow \{\boldsymbol{S} \big| \boldsymbol{S} \in \mathbb{X}^\kappa,\ |Y_{lM+m} - \boldsymbol{\mathcal{H}}_l^m \boldsymbol{S}| \leqslant r\}$;
    Generate a set of current coordinates of nonzero entries: $\mathcal{V}^m \leftarrow \{v | \forall i \in \mathcal{I},\ v \leftarrow (m-i) \bmod M\}$;
    Generate a intersection of the existing and current nonzero coordinates sets: $\mathcal{W}^m \leftarrow \mathcal{U}^m \bigcap \mathcal{V}^m$;
    Construct an injective mapping of coordinates: $f:\ \ell \rightarrow (m-i_\ell) \bmod M, \ell \in \{0, 1, \ldots, \kappa-1\}$;
    for all $\boldsymbol{S} \in \mathcal{S}^m$ **do**
      Generate a set of symbol sequences for a given current $\boldsymbol{S} \in \mathcal{S}^m$:
      $\mathcal{X}_{\boldsymbol{S}}^{m+1} \leftarrow \{\boldsymbol{X}^{m+1} | \boldsymbol{X}^m \in \mathcal{X}^m,\ \forall w \in \mathcal{W}^m,\ X_w^{m+1} = S_{f^{-1}(w)};\ \forall \nu \in \complement_{\mathcal{V}^m} \mathcal{W}^m,\ X_\nu^{m+1} \leftarrow S_{f^{-1}(\nu)}\}$;
      The candidate receives one vote: $\beta_{lM+v}^m(S_{f^{-1}(v)}) \leftarrow \beta_{lM+v}^m(S_{f^{-1}(v)}) + 1, v \in \mathcal{V}^m$;
    end for
    Generate a set of entire symbol sequences for all $\boldsymbol{S} \in \mathcal{S}^m$**:** $\mathcal{X}^{m+1} \leftarrow \bigcup_{\boldsymbol{S}\in\mathcal{S}^m} \mathcal{X}_{\boldsymbol{S}}^{m+1}$;
    Update the existing nonzero coordinates set: $\mathcal{U}^{m+1} \leftarrow \mathcal{U}^m \bigcup \mathcal{V}^m$;
  end for
  if $\mathcal{X}^M = \varnothing$ **then**
    Weighted voting decision symbol-by-symbol: $\widehat{X}_{lM+k} \leftarrow \arg\max_{X\in\mathbb{X}} \sum_{m=0}^{M-1} \frac{\beta_{lM+k}^m(X)}{|\mathcal{S}^m|},\ k \in \{0, 1, \ldots, M-1\}$;
  else
    Maximum likelihood estimation from candidate set: $\widehat{\boldsymbol{X}}_l \leftarrow \arg\min_{\boldsymbol{X}_l^M \in \mathcal{X}^M} \|\boldsymbol{Y}_l - \boldsymbol{\mathcal{H}}_l \boldsymbol{X}_l^M\|_2$;
  end if
end for
return $\widehat{\boldsymbol{X}}$.

$\mathcal{W}^m$ to each symbol sequence $\boldsymbol{X}^m$ and construct $\boldsymbol{X}^{m+1}$. Then, the set $\mathcal{X}_{\boldsymbol{S}}^{m+1}$ is updated accordingly. For each $v \in \mathcal{V}^m$, the candidate $S_{f^{-1}(v)}$ corresponding to the vth entries of symbol vector receives one vote, i.e., $\beta_{lM+v}^m(S_{f^{-1}(v)}) = \beta_{lM+v}^m(S_{f^{-1}(v)}) + 1$.

(3) Repeat Step (2) by enumerating all $\boldsymbol{S} \in \mathcal{S}^m$. Then, the set of entire symbol sequences $\mathcal{X}^{m+1}$ is obtained by the union of all $\mathcal{X}_{\boldsymbol{S}}^{m+1}$. $\mathcal{U}^{m+1}$ is updated to $\mathcal{U}^m \bigcup \mathcal{V}^m$ as the existing nonzero coordinates set for the next iteration.

After M iterations, the set of candidate vectors $\mathcal{X}^M$ can be ultimately obtained. For the candidate $X \in \mathbb{X}$, define the weighted votes as $\sum_{m=0}^{M-1} \frac{\beta_{lM+k}^m(X)}{|\mathcal{S}^m|}$, where $|\mathcal{S}^m|$ is the total number of symbol sequences lying in the sphere radius r and $\beta_{lM+k}^m(X)$ denotes the number of the votes of the candidate X in the mth iteration. If the candidate set $\mathcal{X}^M$ is empty, the weighted voting system estimates the transmitted vector symbol-by-symbol with the most weighted votes. Otherwise, it chooses the transmitted vector $\boldsymbol{X}_l^M \in \mathcal{X}^M$ with the minimum ℓ^2 distance of $\left\|\boldsymbol{Y}_l - \boldsymbol{\mathcal{H}}_l \boldsymbol{X}_l^M\right\|_2$.

It should be emphasized that the PIS decoding method cannot estimate the transmitted vectors when there are no lattice points inside the sphere, i.e., $\mathcal{X}^M = \varnothing$, while the proposed receiver can estimate the transmitted vector with the most weighted votes symbol-by-symbol, and thus, can perform an efficient decoding with the knowledge of the sets $\mathcal{S}^0, \mathcal{S}^1, \ldots, \mathcal{S}^{M-1}$ of the symbol sequences, which have been obtained through PIS decoding. It should be noted that weighted voting can be regarded as a normalization of different candidate symbols, which guarantees $\mathcal{S}^0, \mathcal{S}^1, \ldots, \mathcal{S}^{M-1}$ to make the same contribution to decision.

For a better understanding, we provide a simple example of sparse rotated V-OFDM system with vector size $M = 4$ and the remainder set $\mathcal{I} = \{0, 3\}$. It should be noted that although the channel blocked matrix $\boldsymbol{\mathcal{H}}_l$ in Figure 2 may not be very sparse, it is straightforward to illustrate the updating process of the PIS-WV decoding method. Assume that the binary phase-shift keying (BPSK) modulated symbol vector $\boldsymbol{X}_l = [+1; +1; -1; +1]$ is transmitted through the channel. As the received signals are interfered by noise, after 4 iterations in Algorithm 1, the set of candidate vectors has two elements, i.e., $\mathcal{X}^4 = \{[+1; +1; -1; +1], [-1; +1; -1; +1]\}$. Then, the receiver chooses one element with the minimum ℓ^2

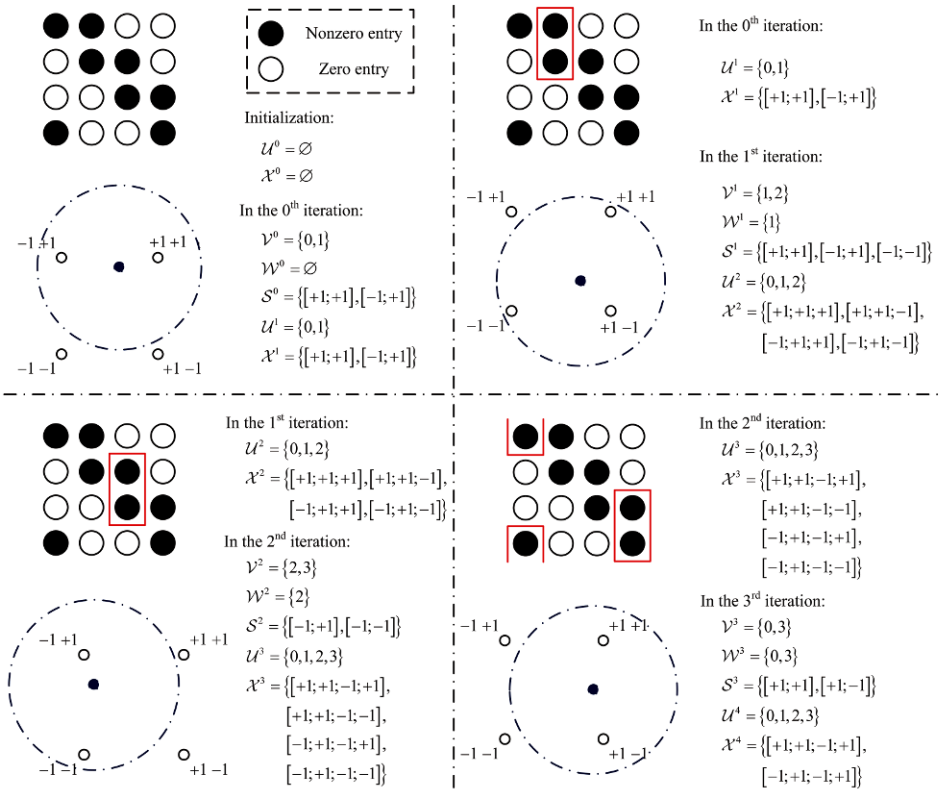

Figure 2 (Color online) Example of the updating process of the partial intersection sphere decoding method.

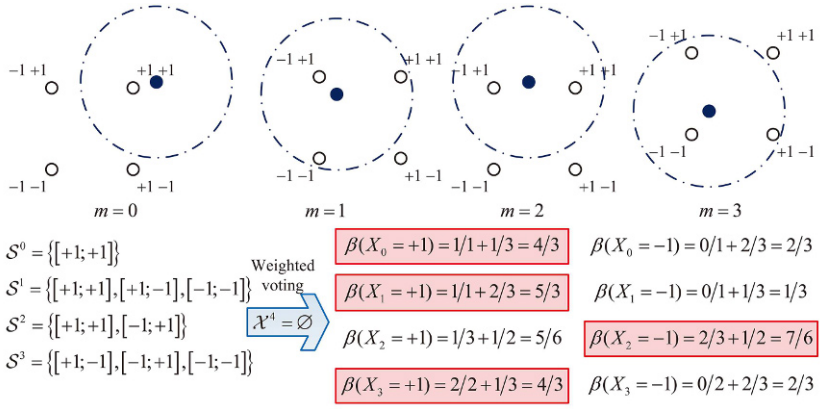

Figure 3 (Color online) Example of the weighted voting system for strong noise scenarios.

distance and obtains $\widehat{\boldsymbol{X}}_l=[+1;+1;-1;+1]$. When the received signals are interfered with strong noise, however, the updating process may generate an empty set of candidate vectors, i.e., $\mathcal{X}^4=\varnothing$, as shown in Figure 3. In this case, based on the knowledge of $\mathcal{S}^0,\mathcal{S}^1,\mathcal{S}^2,\mathcal{S}^3$, the weighted voting system can still make a correct decision on the transmitted vector with the most weighted votes symbol-by-symbol.

It is worth noting that although the PIS-WV decoding method eventually recovers the transmitted vectors $\widehat{\boldsymbol{X}}$, as illustrated in Algorithm 1, the intermediate information can be extended to soft-decision decoding which is more robust to noise. On one hand, once the set $\mathcal{X}^M$ of candidate vectors is generated, the PIS decoding method computes the Euclidean distances $\left\|\boldsymbol{Y}_l-\boldsymbol{\mathcal{H}}_l\boldsymbol{X}_l^M\right\|_2$ for all $\boldsymbol{X}_l^M\in\mathcal{X}^M$. Instead of choosing the transmitted vector from the set $\mathcal{X}^M$ with the minimum distance, for soft-decision decoding, all the $\left|\mathcal{X}^M\right|$ Euclidean metrics are kept as a measurement of the probabilities for the transmitted vector. On the other hand, for an extreme case, such as when a candidate set is empty, i.e., $\mathcal{X}^M=\varnothing$, the

weighted voting system counts the received votes for each candidate symbol. Soft-decision decoding does not decide which candidate symbol receives the most weighted votes, but collects the number of weighted votes as an inclination of the transmitted symbol.

4 Complexity analysis

In this section, we focus on the computational complexity of the proposed PIS-WV decoding method. As is well known, for either sparse or non-sparse channels over a rotated V-OFDM system, the complexities with respect to complex multiplication operation of MMSE decoding and ML decoding are always $\mathcal{O}(LM\log M + LMQ)$ and $\mathcal{O}(LM^2Q^M)$, respectively, where Q stands for the modulation order. For a sparse channel, the complexity of searching possible sequences is only exponential to κ and much less than M. The PIS decoding method needs κLMQ^κ complex multiplication operations in addition to necessary comparison operations varying from κLM to κLMQ^M dependent on the sphere radius r. As the sets of symbol sequences $\mathcal{S}^0, \mathcal{S}^1, \ldots, \mathcal{S}^{M-1}$ have been obtained through PIS decoding, weighted voting only involves $\sum_{m=0}^{M-1} \kappa L \left|\mathcal{S}^m\right|$ integer additions for the count of votes, which is always less than κLMQ^κ complex multiplication operations executed in PIS decoding. For the decision made by maximum likelihood ($\mathcal{X}^M \neq \varnothing$) and weighted voting ($\mathcal{X}^M = \varnothing$), there are $\kappa\left|\mathcal{X}^M\right|$ complex multiplication operations and $M\left|\mathcal{X}^M\right|$ real addition operations involved, respectively.

For a given rotated V-OFDM system that the number of subchannels L and the vector size M are fixed, then the complexity of the proposed PIS-WV decoding varies with the random parameter κ. Recall that κ is the cardinality of the remainder set of multipath time delay modulo vector size. When the maximum multipath excess delay P of sparse channel is sufficiently large, the remainders of the nonzero coordinates modulo M are roughly uniformly distributed at the coordinates $0, 1, \ldots, M-1$. Through mathematical induction, we obtain the following theorem.

Theorem 1. For any given number K of nonzero taps and vector size M, when the maximum time delay P is sufficiently large, the probability mass function of κ approximates to

$$P(\kappa) = \sum_{i=1}^{\kappa} \binom{M}{\kappa}\binom{\kappa}{i}(-1)^{\kappa-i}\left(\frac{i}{M}\right)^K,\ \kappa = 1, 2, \ldots, \min\{K, M\}, \tag{12}$$

where the binomial coefficients $\binom{M}{\kappa} = \frac{M!}{\kappa!(M-\kappa)!}$ and $\binom{\kappa}{i} = \frac{\kappa!}{i!(\kappa-i)!}$, respectively.

Figures 4 and 5 show the probability mass function of κ for different parameters K and M, respectively. In general, with an increases in the number K of nonzero taps and vector size M, the curves of the probability mass function of κ move toward the right hand side direction. On one hand, an increase in the number of nonzero taps K implies an increase in the number of remainder coordinates after taking modulo vector size M with higher probability. On the other hand, for K randomly distributed nonzero coordinates, an increase in vector M implies an increase in candidate remainder coordinates after taking modulo M. As we will see in simulations later, the parameter κ not only has a direct relevance to the decoding complexity, but it also determines the diversity order of PIS-WV decoding over the rotated V-OFDM system.

As the comparison operations cannot be ignored when computing the complexity of PIS-WV decoding, we further investigate the relationship between comparison operations and sphere radius r. $\boldsymbol{S}_\dagger^m$ is denoted as the correct κ-dimensional symbol sequence corresponding to the transmitted symbols, i.e., $\boldsymbol{S}_\dagger^m = \left[X_{lM+(m-i_0) \bmod M}, X_{lM+(m-i_1) \bmod M}, \ldots, X_{lM+(m-i_{\kappa-1}) \bmod M}\right]^{\mathrm{T}}$. Accordingly, the minimum distance $d_{\min}^m$ among all the lattices points in the mth iteration is defined as $\min_{\boldsymbol{S}\in\mathbb{X}^\kappa, \boldsymbol{S}\neq\boldsymbol{S}_\dagger^m}\left|\boldsymbol{\mathcal{H}}_l^m(\boldsymbol{S}-\boldsymbol{S}_\dagger^m)\right|$. Then, we have

$$\begin{aligned}\left|Y_{lM+m} - \boldsymbol{\mathcal{H}}_l^m\boldsymbol{S}\right| &= \left|\boldsymbol{\mathcal{H}}_l^m(\boldsymbol{S}-\boldsymbol{S}_\dagger^m) - (Y_{lM+m} - \boldsymbol{\mathcal{H}}_l^m\boldsymbol{S}_\dagger^m)\right| \\ &\geqslant \left|\boldsymbol{\mathcal{H}}_l^m(\boldsymbol{S}-\boldsymbol{S}_\dagger^m)\right| - \left|Y_{lM+m} - \boldsymbol{\mathcal{H}}_l^m\boldsymbol{S}_\dagger^m\right| \\ &\geqslant d_{\min}^m - \left|Y_{lM+m} - \boldsymbol{\mathcal{H}}_l^m\boldsymbol{S}_\dagger^m\right|. \end{aligned} \tag{13}$$

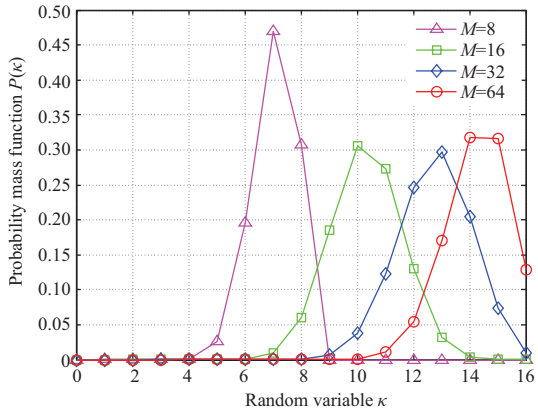

Figure 4 (Color online) Comparison of probability mass function of κ with $K = 16$ and $M = 8, 16, 32, 64$, respectively.

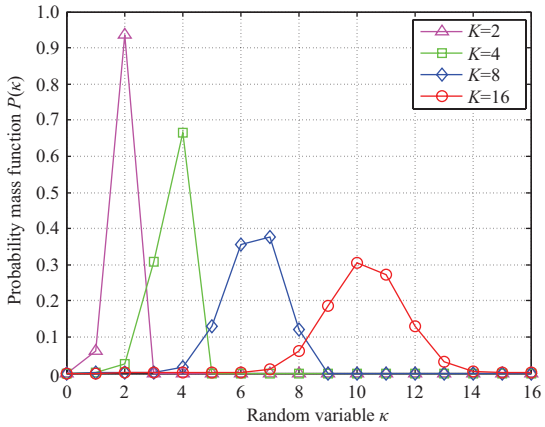

Figure 5 (Color online) Comparison of probability mass function of κ with $M = 16$ and $K = 2, 4, 8, 16$, respectively.

Table 2 All types of operations involved in sphere decoding and PIS-WV decoding for sufficiently high SNR

Decoding method	QR-decomposition	Complex multiplication	Complex comparison	Real addition	Integer addition
Sphere decoding	$2LM^3$	$2LM^2$	$4LM$	$2LM^2$	–
PIS-WV decoding	–	κLMQ^κ	κLM	$M\lvert\mathcal{X}^M\rvert$	$\sum_{m=0}^{M-1}\kappa L\,\lvert\mathcal{S}^m\rvert$

For a given channel $\boldsymbol{h}$ and complex Gaussian noise with variance σ^2, if $d^m_{\min} \geqslant r$, we can further derive that for any $\boldsymbol{S} \in \mathbb{X}^\kappa$ with $\boldsymbol{S} \neq \boldsymbol{S}^m_\dagger$,

$$\Pr\left\{\left|Y_{lM+m} - \boldsymbol{\mathcal{H}}^m_l \boldsymbol{S}\right| \leqslant r\right\} \leqslant \Pr\left\{\left|Y_{lM+m} - \boldsymbol{\mathcal{H}}^m_l \boldsymbol{S}^m_\dagger\right| \geqslant d^m_{\min} - r\right\} = \mathrm{e}^{-\frac{(d^m_{\min}-r)^2}{\sigma^2}}. \tag{14}$$

Therefore, when the SNR is sufficiently high, by choosing the sphere radius $r \leqslant \min_m d^m_{\min}$, $\Pr\left\{\left|Y_{lM+m} - \boldsymbol{\mathcal{H}}^m_l \boldsymbol{S}\right| \leqslant r\right\}$ approaches 0 for all $m = 0, 1, \ldots, M-1$. It should be noted that if $\Pr\left\{\left|Y_{lM+m} - \boldsymbol{\mathcal{H}}^m_l \boldsymbol{S}^m_\dagger\right| \leqslant r\right\} = 1 - \mathrm{e}^{-(r^2/\sigma^2)}$, then the set $\mathcal{S}^m$ always has only one element $\boldsymbol{S}^m_\dagger$ for high SNR scenarios. In this case, only κ symbols needs to be compared in each iteration, and the total complexity with respect to complex comparison operations can be significantly reduced to κLM. When the SNR is sufficiently high, Table 2 compares all types of operations involved in sphere decoding and PIS-WV decoding for a sufficiently high SNR. As a comparison operation and an addition operation are much faster than a complex multiplication operation, the total complexity of PIS-WV decoding can be expressed as $\mathcal{O}(\kappa LMQ^\kappa)$.

In practice, latency and throughput are two key parameters for choosing a parallel and pipeline design for symbol decoding. Processing latency is measured by the elapsed time from the beginning when the signal is received to the end when the decoding is completed. The time flow of PIS-WV decoding is shown in Figure 6. With parallel computing, the symbol decoding of different subchannels can be performed simultaneously. Without loss of generality, we take the lth subchannel as an example. Considering the dependency of process elements, it is found that the set $\mathcal{X}^M$ of candidate vectors and the weighted votes $\boldsymbol{\beta}$ are only dependent on the sets $\mathcal{S}^0, \mathcal{S}^1, \ldots, \mathcal{S}^{M-1}$ of κ-dimensional symbol sequences. In other words, weighted voting can be performed in parallel with the update process of the set $\mathcal{X}^M$; thus, the weighted voting system does not increase additional processing latency compared with PIS-only decoding. On the other hand, the processing throughput is proportional to the number of subchannels, but inversely proportional to the latency of the processing element with the highest latency, which is also known as the critical element. The critical element for PIS-WV decoding is to generate the set $\mathcal{S}^m$ of κ-dimensional symbol sequences.

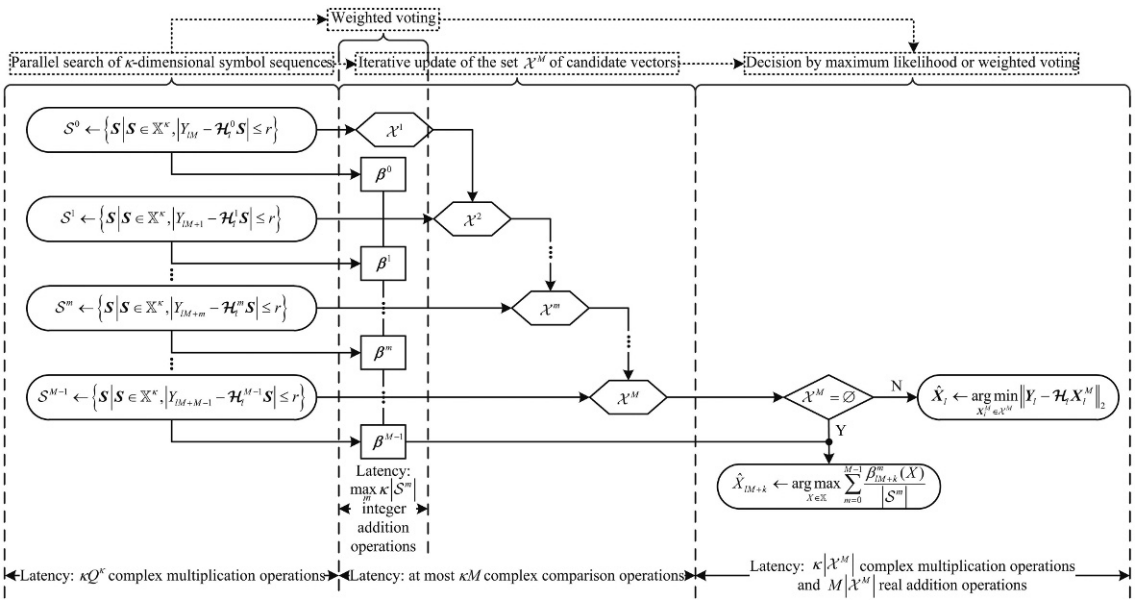

Figure 6 Time flow of PIS-WV decoding for rotated V-OFDM system. The lth subchannel is taken as an example.

5 Numerical results

In the broadband rotated V-OFDM system, a sparse multipath channel $\boldsymbol{h}$ is modeled as K i.i.d. complex Gaussian distributed nonzero taps $h_j \sim \mathcal{CN}(0,1)$, $j \in \mathcal{J}$, randomly distributed within the maximum multipath excess delay P. The symbol sequence is interfered by AWGN and the transmitted SNR $\rho = \frac{1}{\sigma^2}$. The phase-shift keying (PSK) and quadrature amplitude modulation (QAM) are considered in the rotated V-OFDM modulation. We first compare the SERs of different constellation rotations. Then, an example of 3 different channels with deterministic multipath delays is provided to show the diversity order. Furthermore, the proposed PIS-WV decoding method is compared with the conventional ML, zero-forcing (ZF), MMSE, and sphere decoding (SD) methods for a rotated V-OFDM system. Finally, we investigate the decoding complexities for different receivers and their relations to SNR.

Figure 7 shows the SERs of BPSK/QPSK modulated V-OFDM systems with different constellation rotations. Suppose $K = 4$, $L = 4$, $M = 8$, $P = 15$, $r = 1$. We consider V-OFDM systems without rotation, with the rotation suggested in [18], and the proposed parallel rotation, respectively. It can be seen that the rotated V-OFDM outperforms the conventional V-OFDM system, which implies that all the subchannels in rotated V-OFDM can collect full multipath diversity. Furthermore, the SER of the proposed rotation is comparable to the rotation suggested in [18], where the constellation in each subchannel needs to be specifically designed and rotated, whereas the proposed rotation reduces the hardware complexity, as all transmitted vectors are parallel through the same rotation matrix.

In Figure 8, in order to clarify the overlapping of the multipath coordinates after modulo vector size, we adopt the power delay profile model to investigate the diversity orders of 3 different sparse channels with deterministic multipath delays, i.e., Channel A: $\mathcal{J}_A = \{0\}$, Channel B: $\mathcal{J}_B = \{0, 8\}$, Channel C: $\mathcal{J}_C = \{0, 11\}$. Suppose $L = 32$, $M = 8$, $r = 1$. Then, the remainder of multipath delays modulo M for Channel A: $\mathcal{I}_A = \{0\}$, Channel B: $\mathcal{I}_B = \{0\}$, Channel C: $\mathcal{I}_C = \{0, 3\}$. Simulation result indicates that despite $|\mathcal{J}_B| = |\mathcal{J}_C|$, Channel A and Channel B have the same diversity order, which is different from Channel C. Thus, the diversity order is determined by the cardinality of remainder multipath delays set after modulo M, rather than the cardinality of multipath delays set itself.

Figure 9 shows the SERs of different receivers in a rotated V-OFDM system with BPSK modulation. Suppose $K = 4$, $L = 64$, $M = 8$, $P = 15$, and the nonzero taps in a sparse channel are randomly distributed within the maximum multipath excess delay. For fairness of comparison, the sphere radii of PIS-WV and sphere decoding remain 1. Unlike sphere decoding, which cannot estimate the transmitted

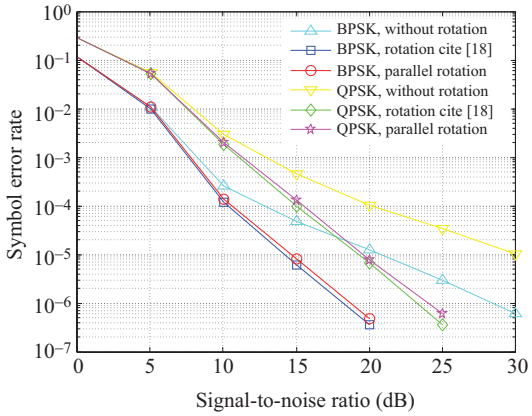

Figure 7 (Color online) Comparison of V-OFDM system with different rotation angles.

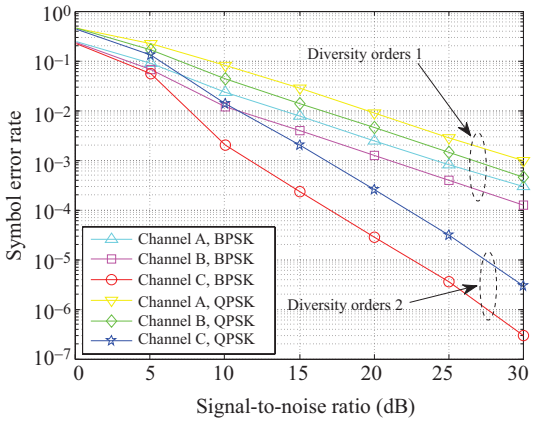

Figure 8 (Color online) Diversity orders of PIS-WV decoding for power delay profile.

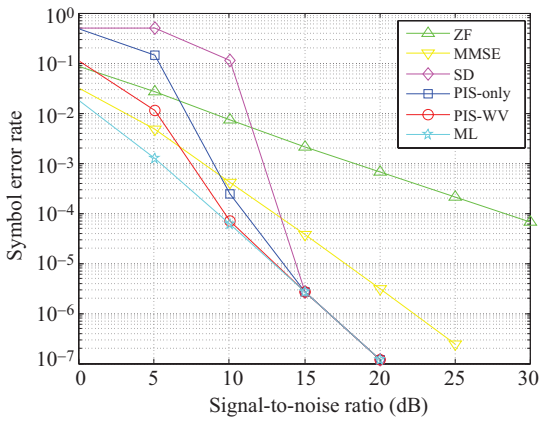

Figure 9 (Color online) Symbol error rates of different receivers over sparse rotated V-OFDM system.

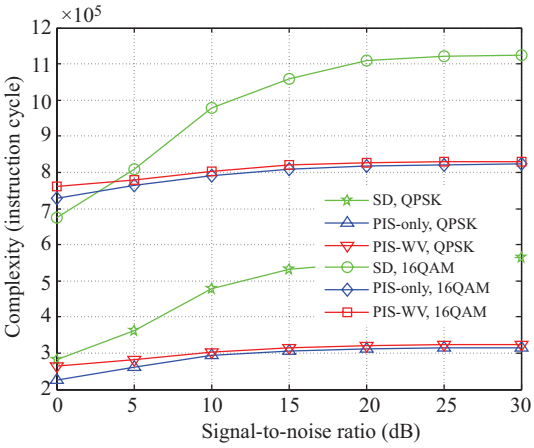

Figure 10 (Color online) Decoding complexities of different receivers over sparse rotated V-OFDM system.

vector when there are no lattice points inside the sphere, i.e., $\mathcal{X}^M = \varnothing$, the proposed PIS-WV decoding method estimates the transmitted vector symbol-by-symbol with the most weighted votes. As a result, PIS-WV decoding outperforms sphere decoding and PIS-only decoding, especially at a low SNR. With an increase of the SNR, PIS-WV decoding improves the SER performance compared with ZF decoding and MMSE decoding, and gradually approaches ML decoding. Furthermore, the diversity orders of the ML and MMSE receivers are equal to 2 (corresponding to the minimum κ), which is in accordance with the results in [18, 21].

Figure 10 compares the decoding complexities of different receivers in a rotated V-OFDM system with QSPK and 16QAM modulations. In assembly language, a comparison operation or an addition operation usually executes 1 instruction cycle, whereas a real multiplication operation executes 4 instruction cycles or slightly more owing to hardware. We consider all types of operations involved in proposed PIS-WV decoding, i.e., complex multiplication operations, complex comparison operations, integer addition operations, and real addition operations. For higher modulation order, by taking advantage of the special structure of $\boldsymbol{\mathcal{H}}_l$, we can save the results of $\boldsymbol{\mathcal{H}}_l^m \boldsymbol{S}$, $\forall \boldsymbol{S} \in \mathbb{X}^\kappa$, $m = i_0, i_1, \ldots, i_{\kappa-1}$ when generating the set of possible symbol sequences such that the complexity can be further reduced. Suppose $K = 2$, $L = 64$, $M = 8$, $P = 15$, $r = 1$, and the nonzero taps in a sparse multipath channel are randomly distributed within the maximum multipath excess delay. It is shown that the average complexities of sphere decoding, PIS-only decoding, and PIS-WV decoding increase with SNR as more entries in the set of possible symbol

sequences are updated with probability in each iteration. For a low SNR, PIS-WV decoding is slightly more complex than PIS-only decoding, as the weighted voting system needs to be executed with high probability. Compared with sphere decoding, the proposed PIS-WV decoding method can reduce the complexity by taking advantage of the sparse nature of a multipath channel.

6 Conclusion

In this paper, an efficient PIS-WV decoding method has been proposed for a sparse rotated V-OFDM system. Unlike ML decoding that requires the enumeration of symbol constellation, the proposed PIS-WV decoding method chooses the transmitted vector only from the set of candidate vectors with the ML estimation generated through PIS decoding. For an extreme case, such as when a candidate set is empty, a weighted voting system is used to estimate the transmitted vector symbol-by-symbol with the most weighted votes. For a rotated V-OFDM system, the proposed PIS-WV decoding method improves the SER performance with reduced complexity, especially for low SNR scenarios. It is worth noting that the PIS-WV decoding can be extended to soft-decision decoding that is more robust to noise.

Acknowledgements This work was supported by National Natural Science Foundation of China (Grant No. 61401194), China Scholarship Council (Grant No. 201406190083), and Program B for Outstanding Ph.D. Candidate of Nanjing University (Grant No. 201501B013).

Conflict of interest The authors declare that they have no conflict of interest.

References

1 Cimini L J. Analysis and simulation of a digital mobile channel using orthogonal frequency division multiplexing. IEEE Trans Commun, 1985, 33: 665–675
2 Astély D, Dahlman E, Furuskär A, et al. LTE: the evolution of mobile broadband. IEEE Commun Mag, 2009, 47: 44–51
3 Hwang T, Yang C, Wu G, et al. OFDM and its wireless applications: a survey. IEEE Trans Veh Tech, 2009, 58: 1673–1694
4 Daoud O. Performance improvement of wavelet packet transform over fast Fourier transform in multiple-input multiple-output orthogonal frequency division multiplexing systems. IET Commun, 2012, 6: 765–773
5 Zhang T X, Xia X-G, Kong L J. CP-based MIMO OFDM radar IRCI free range reconstruction using real orthogonal designs. Sci China Inf Sci, 2017, 60: 022301
6 Wang N, Blostein S D. Comparison of CP-based single carrier and OFDM with power allocation. IEEE Trans Commun, 2005, 53: 391–394
7 Tajer A, Nosratinia A. Diversity order in ISI channels with single-carrier frequency-domain equalizers. IEEE Trans Wirel Commun, 2010, 9: 1022–1032
8 Souto N, Dinis R, Silva J C. Impact of channel estimation errors on SC-FDE systems. IEEE Trans Commun, 2014, 62: 1530–1540
9 Falconer D, Ariyavisitakul S L, Benyamin-Seeyar A, et al. Frequency domain equalization for single-carrier broadband wireless systems. IEEE Commun Mag, 2002, 40: 58–66
10 Pancaldi F, Vitetta G, Kalbasi R, et al. Single-carrier frequency-domain equalization. IEEE Signal Process Mag, 2008, 25: 37–56
11 Xia X-G. Precoded and vector OFDM robust to channel spectral nulls and with reduced cyclic prefix length in single transmit antenna systems. IEEE Trans Commun, 2001, 25: 1363–1374
12 Zhang H, Xia X-G, Zhang Q, et al. Precoded OFDM with adaptive vector channel allocation for scalable video transmission over frequency selective fading channels. IEEE Trans Mobile Comput, 2002, 1: 132–141
13 Zhang H, Xia X-G, Cimini L J, et al. Synchronization techniques and guard-band-configuration scheme for single-antenna vector-OFDM systems. IEEE Trans Wirel Commun, 2005, 4: 2454–2464
14 Zhang H, Xia X-G. Iterative decoding and demodulation for single-antenna vector OFDM systems. IEEE Trans Veh Tech, 2005, 55: 1447–1454
15 Zhou W, Fan L, Chen H. Vector orthogonal frequency division multiplexing system over fast fading channels. IET Commun, 2014, 8: 2322–2335
16 Ngebani I, Li Y, Xia X-G, et al. Analysis and compensation of phase noise in vector OFDM systems. IEEE Trans Signal Process, 2014, 62: 6143–6157
17 Ngebani I, Li Y, Xia X-G. EM-based phase noise estimation in vector OFDM systems using linear MMSE receivers. IEEE Trans Veh Tech, 2016, 65: 110–122

18 Han C, Hashimoto T, Suehiro N. Constellation-rotated vector OFDM and its performance analysis over Rayleigh fading channels. IEEE Trans Commun, 2010, 58: 828–838
19 Han C, Hashimoto T. Tight PEP lower bound for constellation-rotated vector-OFDM under carrier frequency offset and fast fading. IEEE Trans Commun, 2014, 62: 1931–1943
20 Cheng P, Tao M, Xiao Y, et al. V-OFDM: on performance limits over multi-path Rayleigh fading channels. IEEE Trans Commun, 2011, 59: 1878–1892
21 Li Y, Ngebani I, Xia X-G. On performance of vector OFDM with linear receivers. IEEE Trans Signal Process, 2012, 60: 5268–5280
22 Kannu A P, Schniter P. On communication over unknown sparse frequency-selective block-fading channels. IEEE Trans Inf Theory, 2011, 57: 6619–6632
23 Salous S, Degli Esposti V, Fuschini F, et al. Millimeter-wave propagation. IEEE Trans Inf Theory, 2016, 58: 115–127
24 Wang G, Liao H, Wang H. Systematic and optimal cyclotomic lattices and diagonal space-time block code designs. IEEE Trans Inf Theory, 2004, 50: 3348–3360
25 Agrell E, Eriksson A, Vardy A, et al. Closest point search in lattices. IEEE Trans Inf Theory, 2002, 48: 2201–2214
26 Studer C, Burg A, Bölcskei. Soft-output sphere decoding: algorithms and VLSI implementation. IEEE J Sel Areas Commun, 2008, 26: 290–300
27 Hassibi B, Vikalo H. On the sphere decoding algorithm I. Expected complexity. IEEE Trans Signal Process, 2005, 53: 2806–2818
28 Vikalo H, Hassibi B. On the sphere decoding algorithm II. Generalizations, second-order statistics, and applications to communications. IEEE Trans Signal Process, 2005, 53: 2819–2834
29 Jaldén J, Ottersten B. On the complexity of sphere decoding in digital communications. IEEE Trans Signal Process, 2005, 53: 1474–1484
30 Seethaler D, Jaldén J, Studer C, et al. On the complexity distribution of sphere decoding. IEEE Trans Inf Theory, 2011, 57: 5754–5768